Supporting information

Simultaneous elimination of toxic dyes, ciprofloxacin and Cr (VI) contents from polluted water: Escalating Surface plasmon electrons of Ag cocatalysts on $BiVO_4$ microstructures†

Muhammad Zeeshan Abid[a], Asfa Ilyas[a], Khezina Rafiq[a]*, Abdul Rauf[a], Muhammad Arif Nadeem[b], Amir Waseem[b], Ejaz Hussain[ab]*

[a]Institute of Chemistry, Inorganic Materials Laboratory 52S, The Islamia University of Bahawalpur-63100, Pakistan
[b]Catalysis and Nanomaterials Lab 27, Department of Chemistry, Quaid-i-Azam University, Islamabad 45320, Pakistan

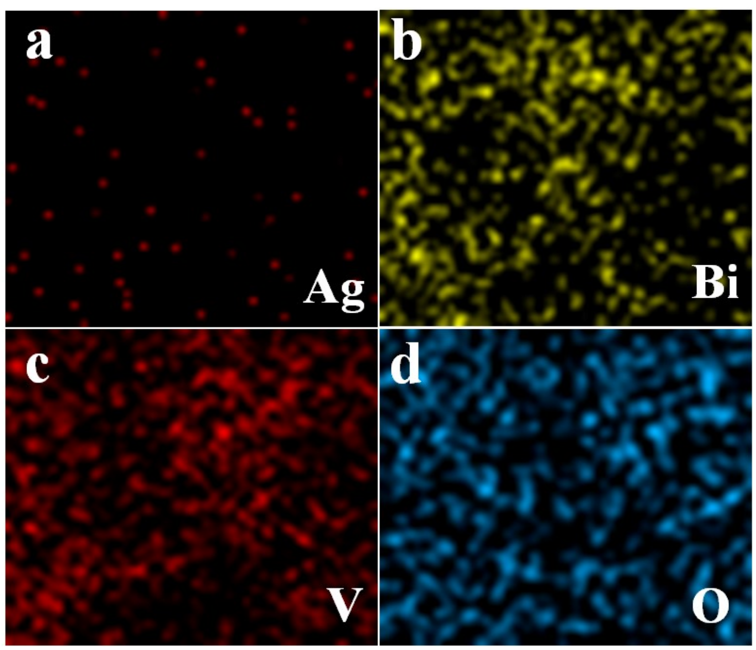

Figure S1: Elemental mapping of Ag-$BiVO_4$.

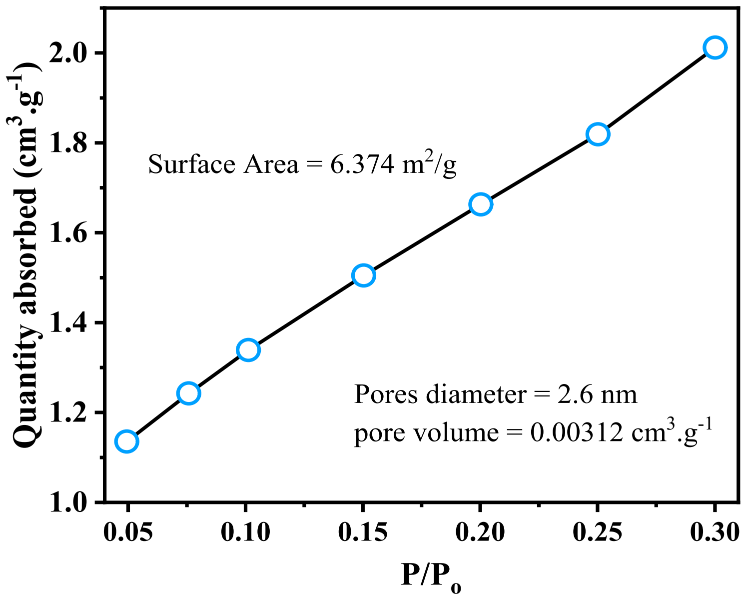

Figure S2: BET, N_2 adsorption-desorption isotherm.

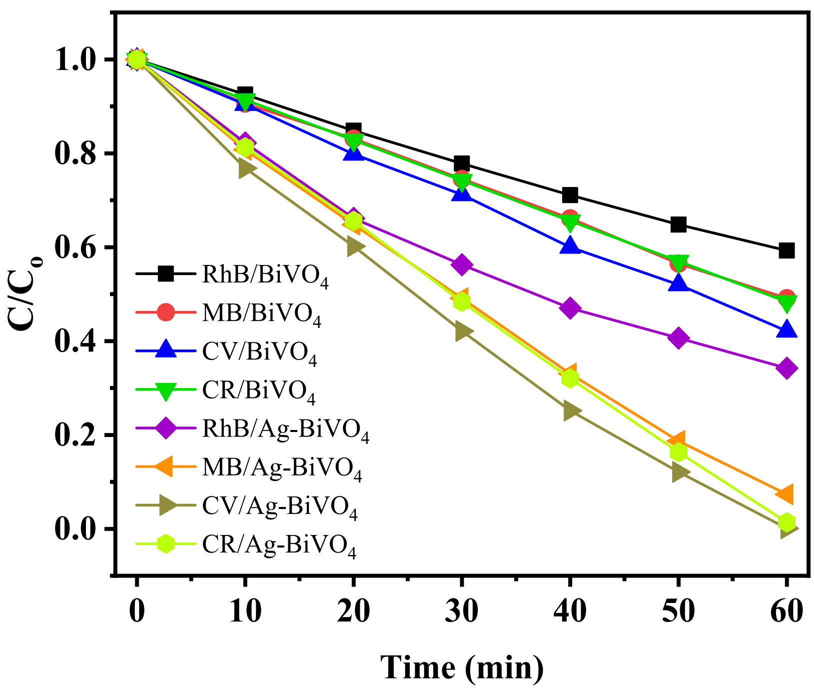

Figure S3: Comparison of RhB, MB, CV and CR dyes degradation with $BiVO_4$ and Ag-$BiVO_4$ photocatalysts.

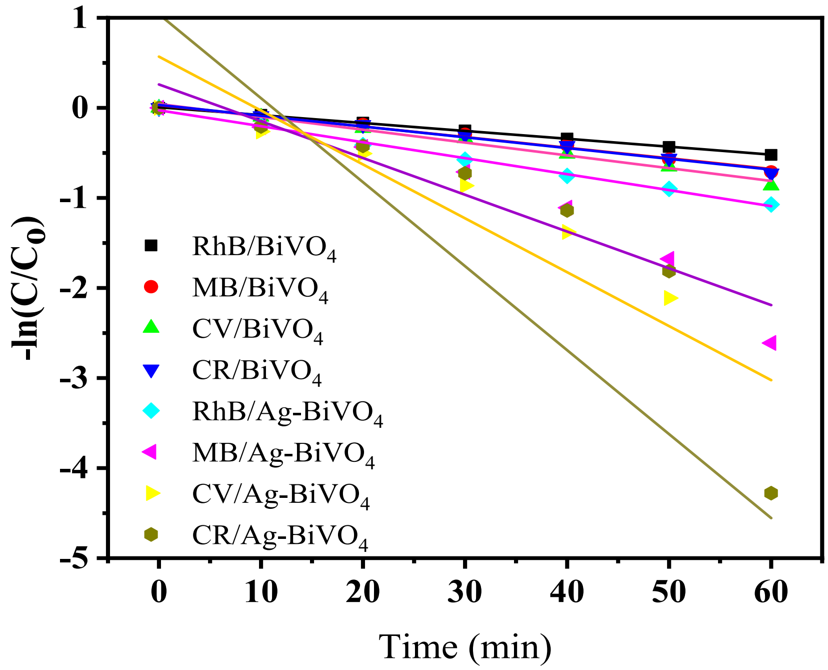

Figure S4: Reaction rates of RhB, MB, CV and CR dyes degradation with $BiVO_4$ and Ag-$BiVO_4$ photocatalysts.

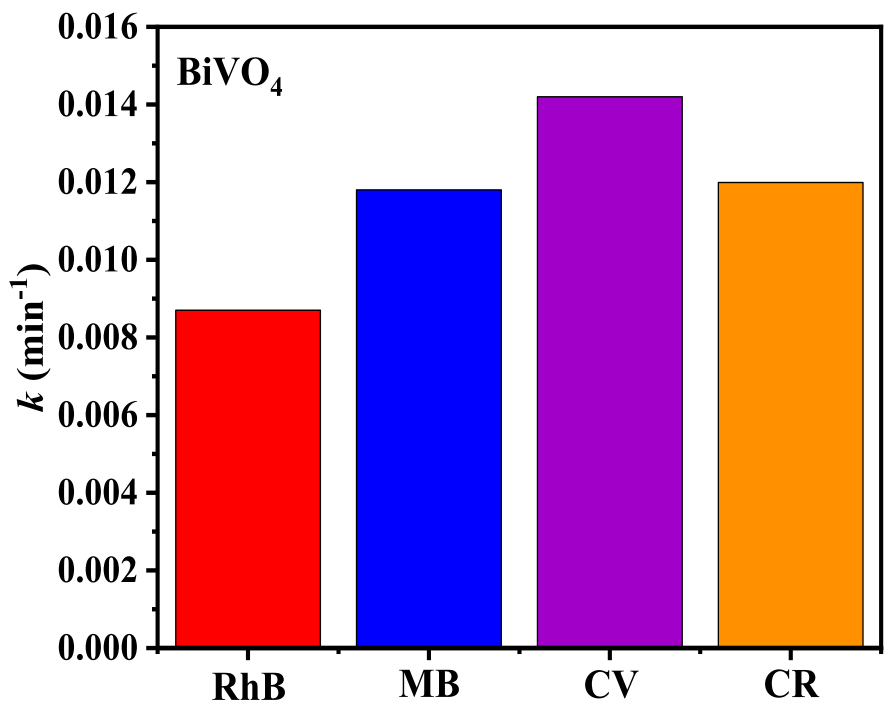

Figure S5: Comparisons of reaction rates of RhB, MB, CV and CR dyes degradation with $BiVO_4$

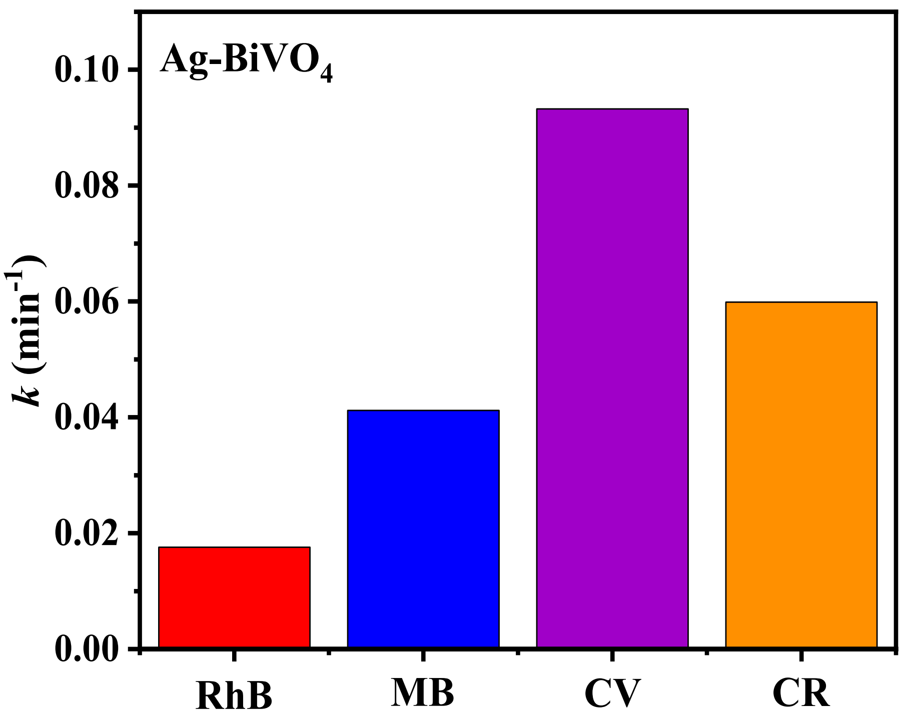

Figure S6: Comparisons of reaction rates of RhB, MB, CV and CR dyes degradation with Ag-$BiVO_4$

Table S1: Physical properties of Methylene Blue

Parameters	**Values**
Chemical formula	$C_{16}H_{18}ClN_3S$
Molar Mass	319.85 g/mol
Appearance	Dark green crystals but appears blue when dissolve
Melting point	100-110 °C
Other name	Basic blue 9
λmax	664 nm
IUPAC name	3,7-bis(Dimethylamino)-phenothiazine-5-ium chloride

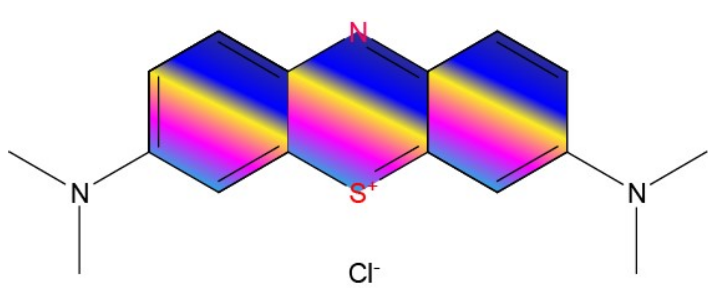

Figure S7: Structure of Methylene Blue

Table S2: Physical properties of Rhodamine B

Parameters	Values
Chemical formula	$C_{28}H_{31}ClN_2O_3$
Molar Mass	479.02 g/mol
Appearance	Red to violet powder
Melting point	210-211 °C
Other name	Rhodamine 610, Pigment violet 1, Basic violet 10
λmax	554 nm
IUPAC name	9-(2-Carboxyphenyl)-6-(diethylamino)-N,N-diethyl-3H-xanthen-3-iminium chloride

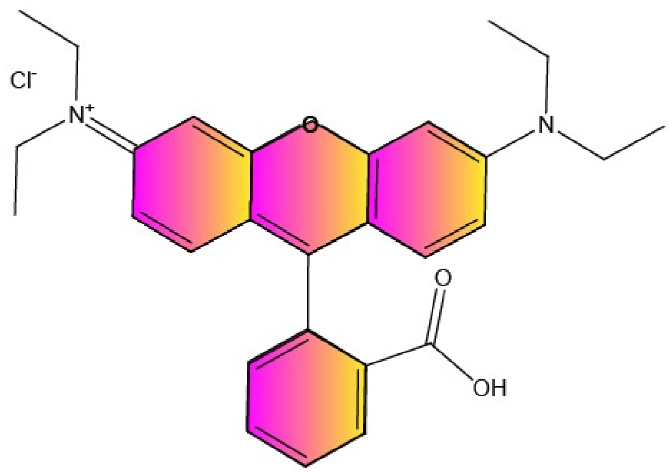

Figure S8: Structure of Rhodamine B

Table S3: Physical properties of Congo red

Parameters	Values
Chemical formula	$C_{32}H_{22}N_6Na_2O_6S_2$
Molar Mass	696.665 g/mol
Appearance	Blue-violet at pH 3.0 and red at pH 5.0
Melting point	>360 °C
λmax	496 nm
IUPAC name	Disodium 4-amino-3-[4-[4-(1-amino-4-sulfonato-naphthalen-2-yl)diazenylphenyl]phenyl]diazenyl-naphthalenr-1-sulfonate

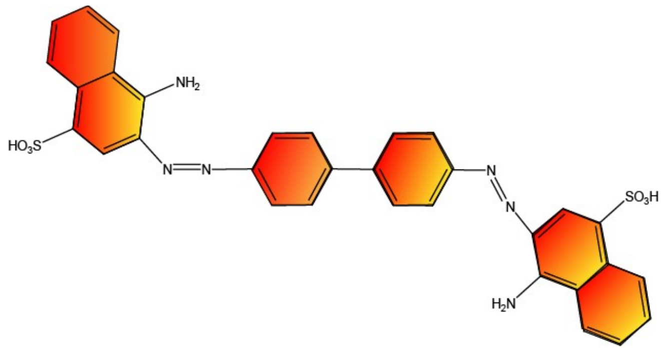

Figure S9: Structure of Congo red

Table S4: Physical properties of Crystal Violet

Parameters	**Values**
Chemical formula	$C_{25}H_{30}ClN_3$
Molar Mass	407.99 g/mol
Appearance	Dark green but appears purple when dissolve
Melting point	205 °C
Other name	Gentian violet, Aniline violet, methyl violet 10B
λmax	590 nm
IUPAC name	4-[1]-N,N-dimethylcyclohexa-2,5-diene-1-iminium chloride

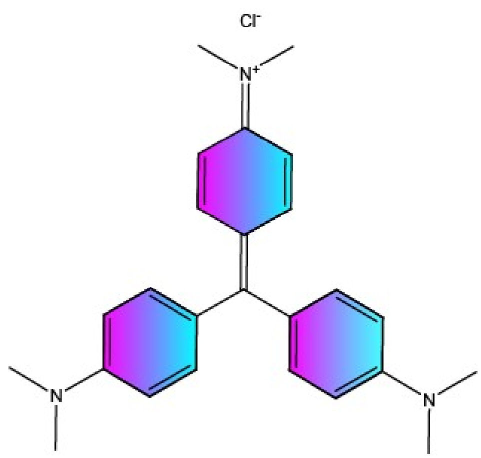

Figure S10: Structure of Crystal Violet

Table S5: Physical properties of ciprofloxacin

Parameters	Values
Chemical formula	$C_{17}H_{18}FN_3O_3$
Molar Mass	331.347 g/mol
Other names	Ciloxan, Cipro, Neofloxin
Melting point	581.8 °C
Appearance	Light yellow crystalline substance
λmax	273 nm
IUPAC name	1-cyclopropyl-6-fluoro-4-oxo-7-piperazin-1-ylquinoline-3-carboxylic acid

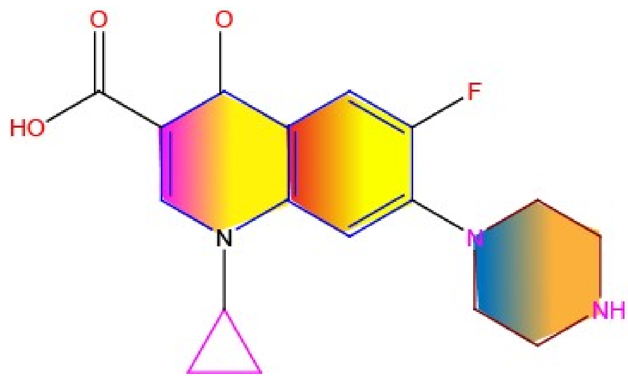

Figure S11: Structure of ciprofloxacin

Table S6: EDX analysis wt% of elements.

Element	Apparent Concentration	K ratio	Wt %	Weight % Sigma
C	0.81	0.00807	4.56	1
O	6.23	0.02098	16.68	1.32
V	6.57	0.06571	13.76	0.72
Ag	0.94	0.00943	2.19	0.83
Au	0.41	0.00412	1.10	0.38
Bi	27.12	0.26523	61.71	1.55
Total:			100	

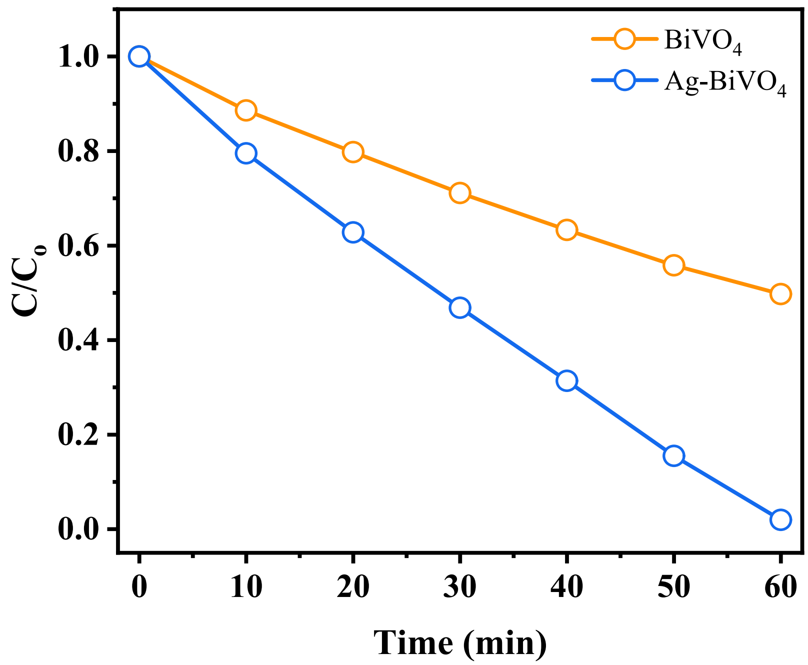

Figure S12: CIP degradation by using $BiVO_4$ and $Ag-BiVO_4$.

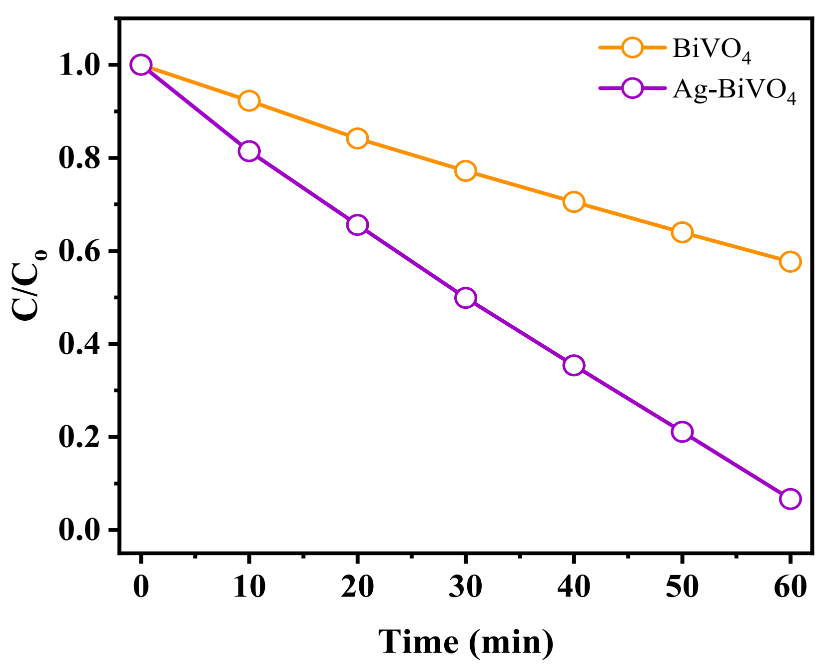

Figure S13: Cr (VI) reduction to Cr (III) by using $BiVO_4$ and $Ag-BiVO_4$.

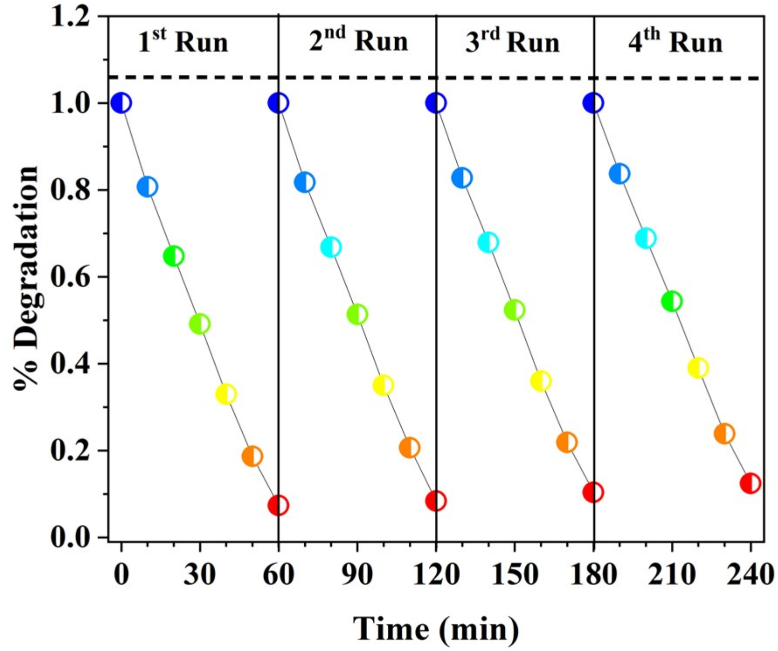

Figure S14: Recyclability of Ag-$BiVO_4$ for MB degradation.

Effect of catalyst dose:

The impact of photocatalyst dosage on the degradation of MB was investigated using 5.0–25 mg of Ag-$BiVO_4$ photocatalyst. Each photoreaction was conducted for 60 min. With an increase in photocatalyst dosage, the degradation rate of MB also increased. This can be attributed to the amplified generation of $^{\bullet}O_2^-$ and $^{\bullet}OH$ radicals, resulting from a greater number of catalytically active sites created by the higher catalyst dosage. However, beyond 20 mg, there was a decline in the degradation rate due to excessive catalyst presence impeding light penetration. These findings are depicted in Figure S15. Therefore, 20 mg was selected as the optimal catalyst dosage for the experiment.

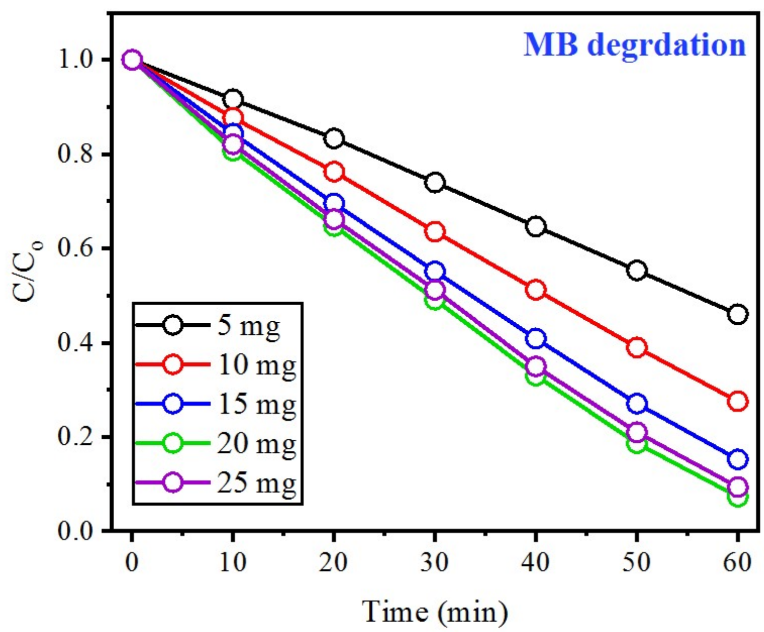

Figure S15: The influence of catalyst dose on the MB degradation via Ag-$BiVO_4$

Sampling from the Field Station: The project was aimed to estimate and remove the hazardous pollutants from the drinking water obtained near to the industrial zones of Pakistan. For the purpose, 20 water samples were collected from the different industrial zones to estimate and remove pollutants (i.e. MB, RhB, CV CR, CIP and Cr(VI)). All collected samples were centrifuged at 5000 rpm for 10 min to remove the suspended particles. The absorbance of each sample was monitored at a UV-VIS spectrophotometer. Although there are various pollutants present but we have targeted the aforementioned pollutants which are present in high concentration and within the detection limit of available instruments. The measured absorption was compared with the standard chart to estimate the concentration of pollutants. The 50 mL of polluted water was treated with 10 mg of as-synthesized Ag-$BiVO_4$ for 10 min to degrade the pollutants. Table S6 represents the estimation and removal of various pollutants collected from industrial drainage, canals, sewage water, and common reservoirs located near to the industrial zones namely Lahore, Faisalabad, Karachi, Multan and Islamabad zones. The survey results depicts that the drinking water collected to the side near to industrial drainage has higher concentrations of pollutants than the samples collected from other water sources of same zone. The detail survey depicts that, concentration of above pollutants in the Karachi industrial zone is high as compared to the other industrial zones of Pakistan.

Table S7: Pollutants degradation from water of various Zones of Pakistan using Ag-$BiVO_4$ catalyst.

Location	Code	Water source	Contaminants	Conc. (ppm)	Abs*	Abs**	% Removal	GPS (Meterk/Handheld-ZL-180)		
								E°	N°	Elev.
Lahore Zone	**LH-1**	Industrial drainage	MB	0.30–0.50	0.08	0.00	100 ± 0.00	74°21'31.4"	31°29'13.3"	220
			RhB	0.10–0.20	0.05	0.00	100 ± 0.00			
			CV	0.10–0.15	0.04	0.00	100 ± 0.00			
	LH-2	Sewage	CIP	0.01–0.02	0.01	0.00	100 ± 0.00	74°20'32.6"	31°32'11.3"	222
			Cr(VI)	0.10–0.30	0.06	0.00	100 ± 0.00			
			CR	0.01–0.02	0.01	0.00	100 ± 0.00			
	LH-3	Canal	CV	0.30–0.50	0.08	**0.01**	100 ± 2.00	74°28'35.4"	31°31'15.3"	218
			Cr(VI)	0.10–0.20	0.03	0.00	100 ± 0.00			
	LH-4	Common reservoir	CV	0.10–0.15	0.03	0.00	100 ± 0.00	74°21'33.2"	31°30'10.3"	224
			Cr(VI)	0.01–0.02	0.01	0.00	100 ± 0.00			
Faisalabad Zone	**F-1**	Industrial drainage	MB	0.40–0.60	0.09	**0.01**	100 ± 2.00	73°8'5.85"	31°40'1.55"	188
			RhB	0.10–0.30	0.05	0.00	100 ± 0.00			
			CV	0.30–0.50	0.08	0.00	100 ± 0.00			
	F-2	Sewage	CIP	0.01–0.02	0.01	0.00	100 ± 0.00	73°1'8.88"	31°44'4.60"	185
			Cr(VI)	0.10–0.15	0.04	0.00	100 ± 0.00			
			CR	0.01-0.02	0.01	0.00	100 ± 0.00			
	F-3	Canal	CV	0.10-0.40	0.05	0.00	100 ± 0.00	73°2'5.66"	31°47'1.31"	187
			Cr(VI)	0.15-0.25	0.05	0.00	100 ± 0.00			
	F-4	Common reservoir	CV	0.30–0.50	0.08	**0.01**	100 ± 1.00	73°8'4.32"	31°35'2.41"	189
			Cr(VI)	0.10–0.20	0.04	0.00	100 ± 0.00			
Multan Zone	**M-1**	Industrial drainage	MB	0.10–0.15	0.03	0.00	100 ± 0.00	71°35'27.4"	30°5'26.84"	128
			RhB	0.01-0.02	0.01	0.00	100 ± 0.00			
			CV	0.10-0.20	0.04	0.00	100 ± 0.00			
	M-2	Canal	MB	0.10-0.20	0.05	0.00	100 ± 0.00	71°22'42.1"	30°4'82.04"	120
			RhB	0.30–0.50	0.08	**0.01**	100 ± 1.00			
			CV	0.10–0.20	0.05	0.00	100 ± 0.00			
	M-3	Common reservoir	MB	0.10–0.15	0.03	0.00	100 ± 0.00	71°32'91.5"	30°6'45.40"	125
			RhB	0.01–0.02	0.01	0.00	100 ± 0.00			
	M-4	Sewage	CV	0.10–0.20	0.05	**0.01**	100 ± 1.00	71°41'29.6"	30°2'44.22"	122
			CIP	0.01–0.02	0.01	0.00	100 ± 0.00			
Karachi Zone	**K-1**	Industrial drainage	MB	0.30–0.50	0.08	**0.01**	100 ± 1.00	67°12'8.43"	25°3'10.10"	128
			RhB	0.10–0.20	0.04	0.00	100 ± 0.00			
			CV	0.10–0.15	0.05	0.00	100 ± 0.00			
	K-2	Canal	CV	0.20–0.50	0.08	**0.01**	100 ± 2.00	67°17'25.3"	25°4'12.15"	132
			CIP	0.10–0.30	0.09	**0.01**	100 ± 2.00			
			RhB	0.10–0.20	0.06	**0.01**	100 ± 1.00			
	K-3	Sewage	CV	0.20–0.50	0.08	**0.01**	100 ± 1.00	67°08'5.33"	25°2'26.08"	125
			CIP	0.01–0.02	0.01	0.00	100 ± 0.00			
			Cr(VI)	0.10–0.15	0.04	0.00	100 ± 0.00			
	K-4	Common reservoir	CIP	0.01–0.02	0.01	0.00	100 ± 0.00	67°00'4.23"	24°8'39.25"	120
			CV	0.10–0.20	0.05	0.00	100 ± 0.00			
Islamabad Zone	**IB-1**	Industrial drainage	CV	0.01–0.03	0.01	0.00	100 ± 0.00	73°10'55.1"	33°39'36.1"	555
			CIP	0.01–0.02	0.01	0.00	100 ± 0.00			
			Cr(VI)	0.01–0.02	0.01	0.00	100 ± 0.00			
	IB-2	Canal	CIP	0.01–0.02	0.01	0.00	100 ± 0.00	73°05'28.7"	33°45'36.1"	550
			CV	0.01–0.02	0.01	0.00	100 ± 0.00			
	IB-3	Sewage	CV	0.10–0.20	0.05	0.00	100 ± 0.00	73°01'82.4"	33°68'36.1"	548
			CIP	0.01–0.02	0.01	0.00	100 ± 0.00			
	IB-4	Common reservoir	CV	0.01–0.02	0.01	0.00	100 ± 0.00	73°20'47.6"	33°25'36.1"	552
			CIP	0.01–0.05	0.02	0.00	100 ± 0.00			

Where, Abs* = absorbance before treatment, Abs** = absorbance after treatment.

Table S8: Comparative analysis of dye degradation efficiency of previously reported $BiVO_4$ photocatalysts with Ag-$BiVO_4$ photocatalysts.

Materials	Dye	% efficiency	Time (min)	(%/min) efficiency	Source	Ref.
$BiVO_4$	MB	50 %	120 min	0.41	UV-Visible	[2]
Paint coated $BiVO_4$	MB	72 %	240 min	0.30	Visible	[3]
$BiVO_4/TiO_2$	MB	85 %	120 min	0.70	Visible	[4]
Polycrystalline $BiVO_4$	CR	55 %	60 min	0.91	Visible	[5]
m-$BiVO_4$	RhB	64.8 %	210 min	0.31	Visible	[6]
$BiVO_4$ (biscuits)	RhB	68 %	270 min	0.25	Visible	[7]
$ZnO/BiVO_4$	RhB	72.7 %	150 min	0.48	Visible	[8]
TiO_2-$BiVO_4$	RhB	79.3 %	300 min	0.26	Sunlight	[9]
$BiVO_4/FeVO_4$	CV	71%	60	1.18	300 W Xe Lamp	[10]
$BiVO_4$/p-MoS_2	CV	69.2%	120	0.57	Visible	[11]
Ag-$BiVO_4$	MB	93.6%	60 min	1.56	Sun-light	Current work
Ag-$BiVO_4$	CR	98.6%	60 min	1.64	Sun-light	Current work
Ag-$BiVO_4$	RhB	65.7**%**	60 min	1.09	Sun-light	Current work
Ag-$BiVO_4$	CV	99.2%	60 min	1.65	Sun-light	Current work

References:

1. F. Chen, Q. Yang, Y. Wang, F. Yao, Y. Ma, X. Huang, X. Li, D. Wang, G. Zeng and H. Yu, Efficient construction of bismuth vanadate-based Z-scheme photocatalyst for simultaneous Cr (VI) reduction and ciprofloxacin oxidation under visible light: Kinetics, degradation pathways and mechanism, *Chemical Engineering Journal*, 2018, 348, 157-170.
2. S. Obregón, A. Caballero and G. Colón, Hydrothermal synthesis of BiVO4: Structural and morphological influence on the photocatalytic activity, *Applied Catalysis B: Environmental*, 2012, 117-118, 59-66.
3. M. Kumar and R. Vaish, Photocatalytic dye degradation using BiVO4–paint composite coatings, *Materials Advances*, 2022, 3, 5796-5806.
4. N. Wetchakun, S. Chainet, S. Phanichphant and K. Wetchakun, Efficient photocatalytic degradation of methylene blue over BiVO4/TiO2 nanocomposites, *Ceramics International*, 2015, 41, 5999-6004.
5. P. Madhusudan, M. V. Kumar, T. Ishigaki, K. Toda, K. Uematsu and M. Sato, Hydrothermal synthesis of meso/macroporous BiVO4 hierarchical particles and their photocatalytic degradation properties under visible light irradiation, *Environmental Science and Pollution Research*, 2013, 20, 6638-6645.
6. M. M. Sajid, N. Amin, N. A. Shad, S. B. khan, Y. Javed and Z. Zhang, Hydrothermal fabrication of monoclinic bismuth vanadate (m-BiVO4) nanoparticles for photocatalytic degradation of toxic organic dyes, *Materials Science and Engineering: B*, 2019, 242, 83-89.
7. Y. Lu, Y.-S. Luo, H.-M. Xiao and S.-Y. Fu, Novel core–shell structured BiVO4 hollow spheres with an ultra-high surface area as visible-light-driven catalyst, *CrystEngComm*, 2014, 16, 6059-6065.
8. S. Singh, R. Sharma, G. Joshi and J. K. Pandey, Formation of intermediate band and low recombination rate in ZnO-BiVO4 heterostructured photocatalyst: Investigation based on experimental and theoretical studies, *Korean Journal of Chemical Engineering*, 2017, 34, 500-510.
9. Y. Wang, N. Lu, M. Luo, L. Fan, K. Zhao, J. Qu, J. Guan and X. Yuan, Enhancement mechanism of fiddlehead-shaped TiO2-BiVO4 type II heterojunction in SPEC towards RhB degradation and detoxification, *Applied Surface Science*, 2019, 463, 234-243.
10. M. M. Sajid, H. Assaedi and H. Zhai, Transition metal vanadates (MVO; M= Bi, Fe, Zn) synthesized by a hydrothermal method for efficient photocatalysis, *Journal of Materials Science: Materials in Electronics*, 2023, 34, 539.
11. P. Singh, S. Sharma and P. Devi, in *Two-Dimensional Materials for Environmental Applications*, Springer, 2023, pp. 299-325.